

## The Recognition of Biological Pesticide Adulteration by Attenuated Total Reflection Infrared Spectroscopy

Li Xiao-ting<sup>1,2</sup>, Wand Dong<sup>1</sup>, Zhu Da-Zhou<sup>3</sup>, Ma Zhi-hong<sup>1</sup>,  
Pan Li-gang<sup>1</sup> and Wang Ji-hua<sup>1,2\*</sup>

<sup>1</sup>Beijing Research Center for Agricultural Standards and Testing, Beijing - 100 097, P. R. China.

<sup>2</sup>School of Agriculture and Biology, Shanghai Jiao Tong University, Shanghai - 200 240, P. R. China.

<sup>3</sup>National Engineering Research Center for Information Technology in Agriculture, Beijing - 100 097, P. R. China.

(Received: 27 September 2013; accepted: 04 November 2013)

**Rapid qualitative and quantitative determination of biological pesticide (Avermectin) adulterated with highly toxic pesticide (Chlorpyrifos) were completed by ATR-FTIR technology. The IR absorbance spectra, the second derivative spectra, the comparative analysis of peak intensity and similarity comparison were used for qualitative analysis. The results showed that with the increase of the proportions of Chlorpyrifos which was adulterated into Abamectin, the number of characteristic absorption peaks belonged to Abamectin decreased, and the peak intensity gradually weakened. Conversely, the number of characteristic absorption peaks attributed to Chlorpyrifos increased, and the peak intensity gradually strengthened. The quantitative prediction models of Abamectin EC adulterated with Chlorpyrifos were established by partial least squares regression method and optimized. And then the external validation sets was used to validate the model performance. The results showed that ATR-FTIR technology can accurately determine the content of Abamectin EC adulterated with Chlorpyrifos. The model of prediction precision was improved through spectrum pretreatment, outliers diagnosis and modeling parameters optimization. In addition, the predicted values and the real values had no significant differences. The determination coefficient ( $R^2$ ) was 99.88%. The root mean square error of calibration (RMSEC), the root mean square error of cross-validation (RMSECV) and the root mean square error of prediction (RMSEP) was 0.44, 0.79 and 0.70, respectively. The present study provided a new method for the rapid identification of biological pesticides mixed with chemical pesticides. It also laid a foundation for the application of ATR-FTIR technology to detect biological pesticides.**

**Key words:** Infrared spectroscopy, Attenuated total reflection, Partial least squares, Biological pesticides, Adulteration.

---

Biological pesticide <sup>[1, 2]</sup> uses the basic principles of mutual promotion and restraint between organisms. It controls the harm of harmful organisms. It can be used for the production of fruit trees, vegetables and other pollution-free foods. Biological pesticides attract much attention because of its broad spectrum, high efficiency, low

toxicity and low residue, environmental compatibility and other good characteristics. However, after a period of practice, biological pesticides gradually left out because of its high cost, slow effect and low insecticidal effect compared with chemical pesticides. Under this situation, some illegal manufacturers adulterated high toxic chemical pesticides in biological pesticides to improve insecticidal action with less cost. Although it improves efficacy and reduces costs, but it damages the real effect of biological pesticides and affect the health of people. So it is

---

\* To whom all correspondence should be addressed.  
Tel.: +86-10-51503488; Fax: +86-10-51503793;  
E-mail: wangjh@nercita.org.cn

urgent to develop a recognition and testing technology for biological pesticide adulteration.

Classical pesticide residue detecting methods include Gas Chromatography (GC), High Performance Liquid Chromatography (HPLC), Gas Chromatography-Mass Spectroscopy (GC-MS), Liquid Chromatography Mass Spectrometry (LC-MS) and so on. These methods have high sensitivity and accuracy, high separation efficiency, good repeatability, high selectivity, and strong discrimination ability<sup>3,4</sup>. There is a wide range of applications of these methods, however they hardly satisfy the requirements of large-scale rapid field screening because of their disadvantages, such as the destruction of samples, the additional pre-treatment, the consumption of time, the pollution of environment, the expensive equipment, and so on<sup>5,6</sup>. At the moment, the mainstream methods of rapid detection are Enzyme Inhibition Method (EIM)<sup>7</sup> and Enzyme Linked Immunoassay (ELISA)<sup>8</sup> which have the advantages of simple operation, low testing costs, short detection time and fast speed, as well as the disadvantages of serious specificity and limited kinds of applicable pesticides. Therefore, it needs to exploit a large-scale, rapid identification method of biological pesticide adulteration.

Infrared spectroscopy technique is one of the effective means of qualitative, quantitative and structural analysis of organic compounds. Compared to other spectroscopic techniques, infrared spectroscopy technique has the advantage that the vast majority of various functional groups of organic compounds will appear corresponding absorption peaks in specific regions of the infrared spectra. And the positions are substantially fixed<sup>9</sup>. The various molecular groups of pesticides, such as P-O, C-Cl, O-H, C-N, C-C, C=C, C=O, CH<sub>3</sub>, have characteristic absorption in infrared spectrum. It determines organic functional groups which present in the unknown samples by measuring the infrared spectrum. Therefore, it lays the spectroscopy foundation to ultimately determine the chemical structure of unknown objects<sup>10</sup>. Although the absorption peaks displace shifting to a certain extent because of the influence of chemical structure and external conditions, but it can still reflect the existence or not of functional groups from the peak information through comprehensively considering the peak

position, peak intensity, peak shape, the number of peaks and the presence of the correlative peaks. It determines the existence or not of compounds or functional groups like identifying the person's fingerprint according to differences of infrared spectra of compounds<sup>11,12</sup>. Thus it is possible to perform qualitative analysis of pesticides according to their functional groups and characteristic absorption peaks in the infrared region. PLS (partial least squares)<sup>13,14</sup> is a kind of multivariate regression analysis method. It becomes a common multivariate calibration method in chemometrics because of its strong ability to extract effective information. It can achieve multi-component detection, classification and identification of pesticides by means of combination of infrared spectroscopy and chemometrics. And then it is possible to perform quantitative analysis of pesticides<sup>15</sup>.

The microscopic technology was applied to fourier transform infrared spectrometer in the early 1980s. So the ATR-FTIR (Attenuated Total Reflectance Fourier Transform Infrared Spectroscopy) technology was born followed<sup>[16]</sup>. In accordance with the principle of the optical transmission, it will occur with the total reflection phenomenon when the angle of light is greater than the critical angle and light transfers from optically denser medium to optically thinner medium. The total reflection not occurs when the light is at the interface, but it produces stationed waves which carry information in the optically thinner medium. This phenomenon is known as the attenuated total reflection. The analysis of compositions is convenient and quick in micro regions by application of ATR. The detection sensitivity can reach nanogram grade, and the diameter of measuring micro region can reach micron grade<sup>17</sup>. The advantages of this method are simple operation and non-destructive analysis, and samples can be basically kept their original state when measure. In addition, there are no special requirements on the size, shape, and the water content of samples. Thus, attenuated total reflection technology is expected to be used for recognition and detection of biological pesticides adulterated with chemical pesticides.

In this study, ATR-FTIR technology was used to detect biological pesticides adulterated with chemical pesticides. Abamectin and

Chlorpyrifos were used as research object. The ATR-IR spectra of Abamectin pure powders, Chlorpyrifos pure powders and Abamectin powders mixed with different proportions of Chlorpyrifos powders were collected respectively. In addition, the qualitative and quantitative analysis of spectra was done. The purpose of this study was to explore the feasibility of qualitative and quantitative detection of biological pesticide Abamectin adulterated with high toxic chemical pesticide Chlorpyrifos by applying ATR-FTIR technology.

## MATERIALS AND METHODS

### Samples and reagents

Abamectin powders, Chlorpyrifos powders were purchased from Beijing Shang Li Fang Joint Chemical Technology Research Institute. Abamectin EC A was purchased from Zhejiang Hai Zheng Chemical Engineering Co., Ltd. (pesticide registration number: PD20082353, product standard card number: GB19337-2003, production batch number: A20110629, production date: 2011.6.29). Abamectin EC B was purchased from Zhejiang Hai Zheng Chemical Engineering Co., Ltd. (pesticide registration number: PD20082353, product standard card number: PD20082353, production batch number: A20120423, production date: 2012.4.23). Chlorpyrifos EC C was purchased from Jiangsu Suzhou Jia Hui Chemical Engineering Co., Ltd. (pesticide registration number: PD20084644, product standard card number: GB19605-2004, production batch number: 2011051302, production date: 2011.05.23, the actual content of was 197 g/L measured by gas chromatograph). Chlorpyrifos EC D was purchased from Jiangsu Suzhou Jia Hui Chemical Engineering Co., Ltd. (pesticide registration number: PD20084644, product standard card number: GB19605-2004, production batch number: 2011092401, production date: 20120312, the actual content of was 179 g/L measured by gas chromatograph). Acetone solutions (spectroscopically pure grade) were purchased from Beijing Chemical Works.

### Instruments and equipments

Fourier transform infrared spectrometer (Model: Spectrum 400, Perkin Elmer, USA), attenuated total reflection attachment, gas chromatography (Model: GC 2010, SHIMADZU,

Japan), analytical balance (Model: XS205, Mettler Toledo, Switzerland, sensitivity: 0.0001 g)

### Data processing

A operation software called Spectrum V6.3.5 from Perkin-Elmer was used to extract IR spectra, and the spectra were processed by the second derivative method to get the second derivative spectra, which were smoothed by 5-point smoothing. The derivative spectrum<sup>[18, 19]</sup> was the obtained IR spectrum processed by differentiation processing. The half-peak width was only 1/3 score of the original spectra in the second derivative spectrum. To a certain extent, it could separate the overlapping peaks on the original spectra, and reduce the peak overlap to improve the resolution of the spectra. The similarity compare of samples was comparatively analyzed in this study. The similarity compare is a qualitative analysis method which is used to calculate the similarity degree between samples. Its principle is based on the mathematical correlation coefficient. The similarity degree is compared between two infrared spectra (or between a series of spectra and a spectral). The similarity compare was analyzed by software Spectrum V6.3.5 of Perkin Elmer. The quantitative analysis of infrared spectrum was conducted by PLS. It was completed by chemometrics software Spectrum Quant + V4.51 of Perkin Elmer. PLS is a chemometric algorithm which is the most widely used in infrared spectrum analysis currently. It can remove the noise, extract the spectral information and solve the problem of spectral collineation effectively<sup>20, 21</sup>. The model effect and prediction accuracy was evaluated by the following parameters, such as the determination coefficient of predictive value and chemical values (the measuring value of standard methods) (The determination coefficient,  $R^2$ ), the root mean square error of calibration (RMSEC), the root mean square error of cross-validation (RMSECV), the root mean square error of prediction (RMSEP)<sup>22, 23</sup>.

### Experimental methods

#### Sample preparation methods of qualitative analysis

Firstly, 0.1g of Avermectin and Chlorpyrifos powders were weighed on the analytical balance and placed into centrifuge tubes, respectively. Then 10 mL of acetone solutions were

add into centrifuge tubes. Finally, the 10000 mg/L of Avermectin and Chlorpyrifos solutions were configured. 1 mL 10000 mg/L of Avermectin and Chlorpyrifos solutions were drawn and placed into other centrifuge tubes. And then 9 mL of the acetone solutions was added. So 1000 mg/L of Avermectin and Chlorpyrifos solutions and were configured. By that analogy, 100 mg/L of Avermectin and Chlorpyrifos solutions and were configured. At last, five 100 mg/L of Abamectin and Chlorpyrifos solutions were mixed together, in which volume percentage (V/V) of Chlorpyrifos solutions were 10%, 20%, 30%, 40%, 50% in turn, and the total volume was 20 mL.

#### Sample preparation methods of calibration set and cross-validation set

Forty seven samples of Avermectin EC adulterated with Chlorpyrifos EC were configured according to the need of model number and actual situation. The range of quality percentage of Chlorpyrifos was 1.0%-38.4%, including 11 samples of AC combination, 12 samples of AD combination, 9 samples of BC combination, 15 samples of BD combination. AC combination were the mixed samples of Avermectin EC A and Chlorpyrifos EC C, AD combination were the mixed samples of Avermectin EC A and Chlorpyrifos EC D, BC combination were the mixed samples of Avermectin EC B and Chlorpyrifos EC C, and BD combination were the mixed samples of Avermectin EC B and Chlorpyrifos EC D. So it prevented the interference of samples of internal linear to model through configuring sample crosswise from different sources.

#### Sample preparation methods of external validation set

Similarly, 17 samples of Avermectin EC

adulterated with Chlorpyrifos EC were configured according to the need of model number and actual situation. The range of quality percentage of Chlorpyrifos was 2.8%-37.9%, including 4 samples of AC combination, 4 samples of AD combination, 7 samples of BC combination, 2 samples of BD combination.

#### Collection of infrared spectra

ATR attachment was used to determine. The samples were added dropwise on the crystal of ATR attachment. The air was used as background. The IR spectrum of reference was collected at 4 cm<sup>-1</sup> spectral resolution and scanned 64 times, with a wavenumber range of 4000-600 cm<sup>-1</sup>. The parameter settings of samples were as same as reference, and scanned 32 times.

## RESULTS AND DISCUSSIONS

### Qualitative analysis of biological pesticide adulteration by ATR-FTIR technology

#### Attenuated total reflection Abamectin and Chlorpyrifos powders

Figure 1 (a) and Figure 1 (b) were the structure schematic of Abamectin and Chlorpyrifos. It could be seen that Abamectin contained C=O, C-O, C-C, C=C, C-H and other molecular groups, while Chlorpyrifos contained C-Cl, C=N, C-N, C=C, C-C, C-O, C-H, P=S, P-O and other molecular groups. It showed that Chlorpyrifos had C-Cl, C=N, C-N, P=S, P-O groups specially, and Abamectin had C=O group specially. So it laid the foundation for analysis based on the different molecular structure of Abamectin and chlorpyrifos.

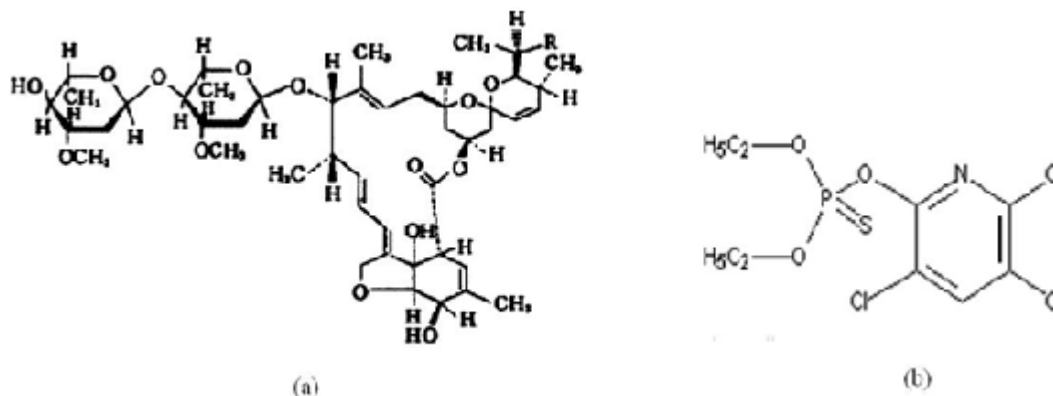
Figure 2 (a), Figure 2 (b) were the ATR-FTIR spectra of Avermectin and Chlorpyrifos.

**Table 1.** Calibration results of MIR by different data preprocess

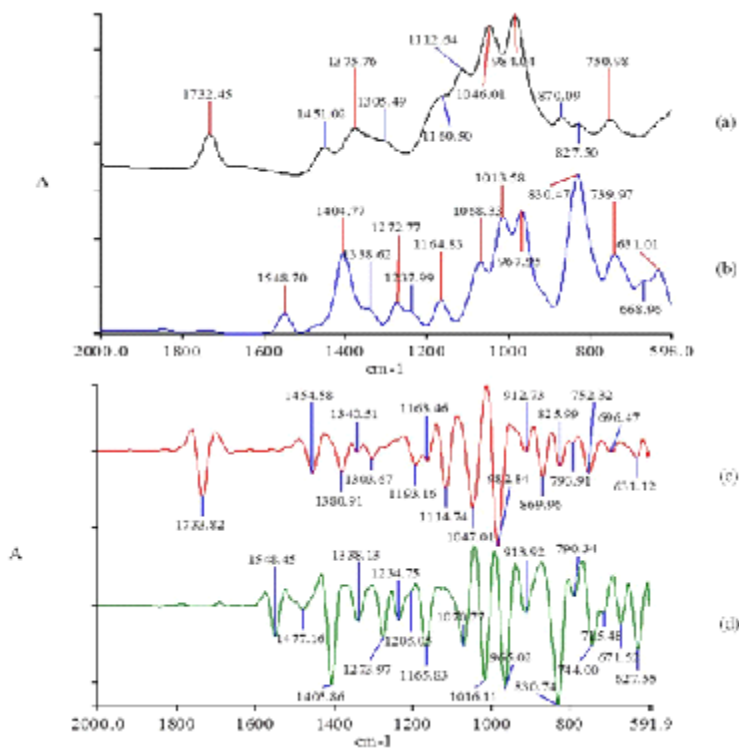
| Number | Centralization | Smoothing | Standardizing | Baseline           | n  | R <sup>2</sup> (%) | RMSEC | RMSECV |
|--------|----------------|-----------|---------------|--------------------|----|--------------------|-------|--------|
| 1      | mean, mean     | N         | N             | N                  | 11 | 99.88              | 0.44  | 0.80   |
| 2*     | mean, mean     | 9         | N             | N                  | 11 | 99.88              | 0.44  | 0.79   |
| 3      | mean, mean     | 13        | N             | N                  | 10 | 99.83              | 0.51  | 0.84   |
| 4      | mean, mean     | 9         | MSC           | N                  | 10 | 99.77              | 0.59  | 0.92   |
| 5      | mean, mean     | 9         | SNV           | N                  | 11 | 99.74              | 0.64  | 0.84   |
| 6      | mean, mean     | 9         | SNV+der       | N                  | 11 | 99.76              | 0.61  | 0.83   |
| 7      | mean, mean     | 9         | N             | 1 <sup>st</sup> -5 | 9  | 99.82              | 0.52  | 1.00   |
| 8      | mean, mean     | 9         | N             | 2 <sup>nd</sup> -5 | 5  | 99.18              | 1.05  | 1.35   |
| 9      | auto, auto     | 9         | N             | N                  | 13 | 99.94              | 0.32  | 0.93   |

Figure 2 (c), Figure 2 (d) were the second derivative spectra corresponding to Figure 2 (a) and Figure 2 (b), respectively. Figure 2 (a), Figure 2 (c) showed that the C=O stretching vibration absorption peak was obvious at  $1735\text{cm}^{-1}$ . In  $1600\text{-}1450\text{ cm}^{-1}$  wavenumber range, there was a heterocyclic ring C=C stretching vibration absorption peak at  $1454.58\text{ cm}^{-1}$ . The three absorption peaks of

different intensity at  $1193.16\text{ cm}^{-1}$ ,  $1163.46\text{ cm}^{-1}$ ,  $1114.74\text{ cm}^{-1}$  corresponded to heterocyclic ring =C-H bending vibration in plane. The characteristic peak at  $1047.01\text{ cm}^{-1}$  associated with C-O stretching vibration. When methyl connected with carbon atoms, the absorption peaks of  $\text{CH}_3$  antisymmetric bending vibration and symmetric bending vibration were at  $1454.58\text{ cm}^{-1}$  and  $1340.51\text{ cm}^{-1}$ . The intensity



**Fig. 1.** The structure schematic of Avermectin single substance (a), The structure schematic of Chlopyrifos single substance (b)



**Fig. 2.** The IR spectrum of Avermectin powders (a), The IR spectrum of Chlopyrifos powders (b), The second derivative spectrum of Avermectin powders (c), The second derivative spectrum of Chlopyrifos powders (d)

of vibration peak at  $1454.58\text{ cm}^{-1}$  was strong, but the intensity of vibration peak at  $1340.51\text{ cm}^{-1}$  was weak. In  $900\text{--}650\text{ cm}^{-1}$  wavenumber range, The absorption peaks of C-H bending vibration out of plane and heterocyclic ring framework vibration were located at  $869.96\text{ cm}^{-1}$ ,  $825.99\text{ cm}^{-1}$ ,  $793.91\text{ cm}^{-1}$ ,  $752.32\text{ cm}^{-1}$  and  $696.47\text{ cm}^{-1}$ <sup>24,25</sup>.

In  $1600\text{--}1450\text{ cm}^{-1}$  wavenumber range, The pyridine ring C=C stretching vibration absorption peaks located at  $1548.45\text{ cm}^{-1}$  and  $1477.16\text{ cm}^{-1}$  (Figure 2 (b) and Figure 2 (d)). The peak at  $1548.45\text{ cm}^{-1}$  was slightly strong, while the peak at  $1477.16\text{ cm}^{-1}$  was weak. A strong absorption peak attributed

to P-O vibration absorption located at  $1273.97\text{ cm}^{-1}$  in  $1300\text{--}1250\text{ cm}^{-1}$  wavenumber range. The moderate absorption peak at  $1234.75\text{ cm}^{-1}$  was from C-O stretching vibration absorption. The absorption peaks at  $1205.05\text{ cm}^{-1}$  and  $1165.83\text{ cm}^{-1}$  corresponded to pyridine ring C-H bending vibration in plane. However, the peak at  $1165.83\text{ cm}^{-1}$  was strong, and the peak at  $1205.05\text{ cm}^{-1}$  was weak. The characteristic absorption peak at  $1070.77\text{ cm}^{-1}$  might be mainly generated by C-Cl. In  $1050\text{--}910\text{ cm}^{-1}$  wavenumber range, there were three strong absorption peaks associated with the P-O-C<sub>2</sub>H<sub>5</sub> at  $1016.11\text{ cm}^{-1}$ ,  $965.02\text{ cm}^{-1}$  and  $913.92\text{ cm}^{-1}$ .

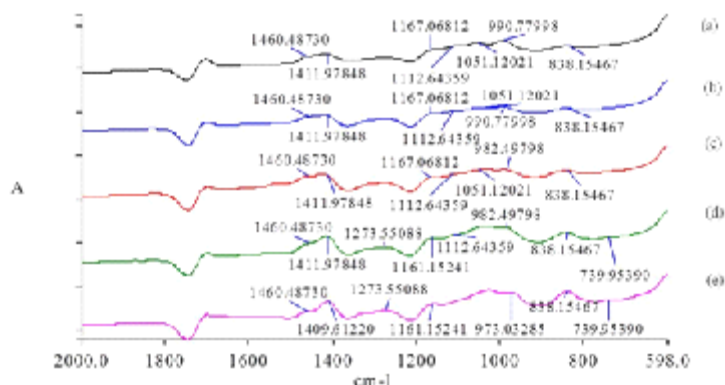


**Fig. 3.** The IR spectrum of 100 mg/L Abamectin solution adulterated 10% (a), 20% (b), 30% (c), 40% (d) and 50% (e) 100 mg/L Chlorpyrifos solution

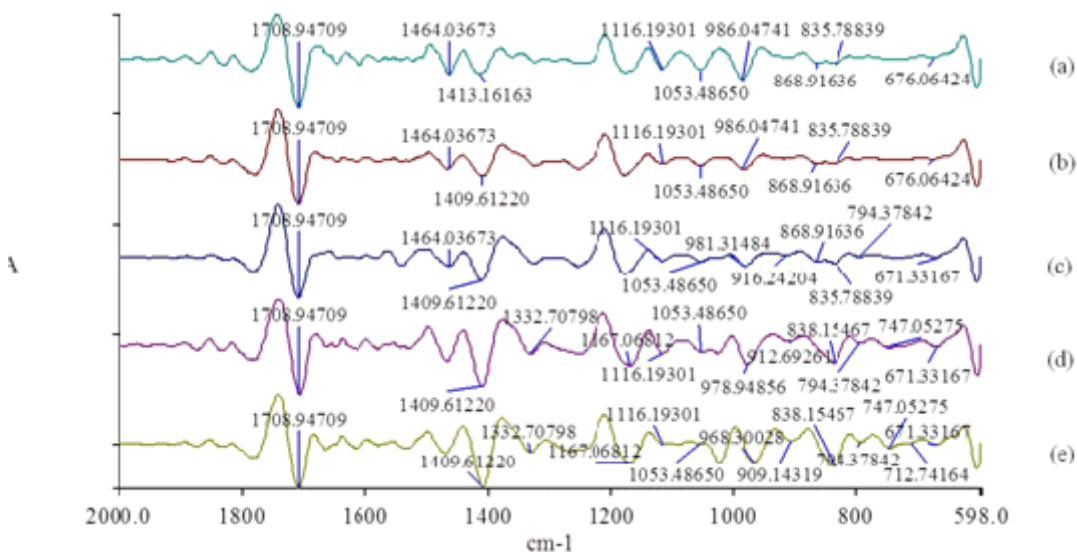


**Fig. 4.** The second derivative spectrum of 100 mg/L Abamectin solution adulterated 10% (a), 20% (b), 30% (c), 40% (d), 50% (e) 100 mg/L Chlorpyrifos solution

These three peaks attributed to the P-O vibration or P-O and C-O vibration coupling. Several absorption peaks of different intensity of C-H pyridine vibration out of plane and pyridine ring framework vibration were located at 830.74  $\text{cm}^{-1}$ , 790.34  $\text{cm}^{-1}$ , 744.00  $\text{cm}^{-1}$ , 715.48  $\text{cm}^{-1}$  and 671.52  $\text{cm}^{-1}$  [25].

The above analysis could suggest the absorption peak of C=O stretching vibration and the absorption peaks of CH<sub>3</sub> antisymmetric bending vibration and symmetric bending vibration only existed in the Abamectin. But the absorption peaks which related to C-Cl, P-O vibration and P-O-C<sub>2</sub>H<sub>5</sub> vibration only existed in the Chlorpyrifos. The differences between the peak position and peak number of Abamectin and Chlorpyrifos were large through analyzing their main molecular

structure and characteristic absorption peaks in the IR spectral region. This provided the basis for the follow-up analysis of Abamectin powders adulterated with Chlorpyrifos powders.

**The analysis of IR spectrum of Avermectin adulteration solution**

Figure 3 (a), Figure 3 (b), Figure 3 (c), Figure 3 (d) and Figure 3 (e) were the IR spectra of 100 mg/L of Abamectin solutions adulterated with 10%, 20%, 30%, 40%, 50% 100 mg/L of Chlorpyrifos solutions. Comparing with the characteristic absorption peaks of Abamectin powders and Chlorpyrifos powders in Figure 2 (a), Figure 2 (b) one by one, it was found that four characteristic absorption peaks of Abamectin at 1460.48  $\text{cm}^{-1}$ , 1112.64  $\text{cm}^{-1}$ , 1051.12  $\text{cm}^{-1}$ , 990.77  $\text{cm}^{-1}$  and three characteristic absorption peaks of Chlorpyrifos at

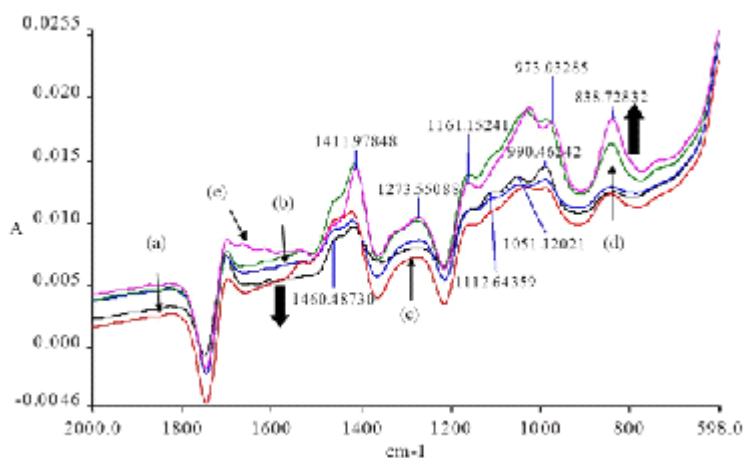


Fig. 5. The IR spectrum of 100 mg/L Abamectin solution adulterated 10% (a), 20% (b), 30% (c), 40% (d) and 50% (e) 100 mg/L Chlorpyrifos solution

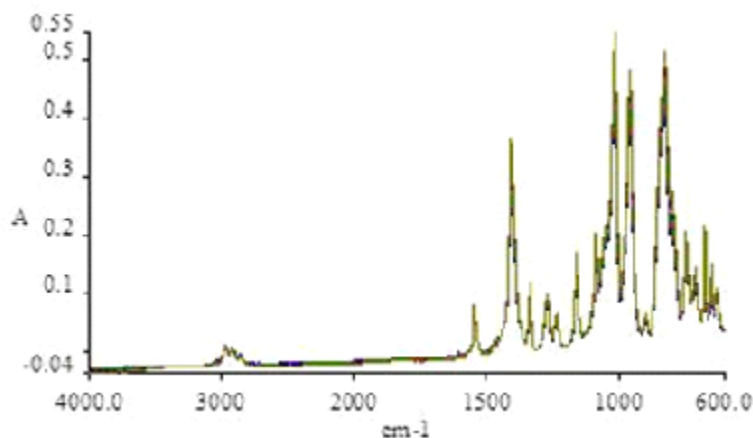


Fig. 6. Ten repeated measure results of MIR spectra of Chlorpyrifos EC C

1411.97  $\text{cm}^{-1}$ , 1167.06  $\text{cm}^{-1}$ , 838.54  $\text{cm}^{-1}$  in Figure 3 (a), respectively. There were four characteristic absorption peaks which belonged to Avermectin in Figure 3 (b), similarly. They were located at 1460.48  $\text{cm}^{-1}$ , 1112.64  $\text{cm}^{-1}$ , 1051.12  $\text{cm}^{-1}$  and 990.77  $\text{cm}^{-1}$  the same. There were the same amount of characteristic absorption peaks which belonged to Chlorpyrifos at the same position in figure 3 (b) as in figure 3 (a). Likewise, it was found four characteristic absorption peaks which attributed to Abamectin at 1460.48  $\text{cm}^{-1}$ , 1112.64  $\text{cm}^{-1}$ , 1051.12  $\text{cm}^{-1}$  and 982.49  $\text{cm}^{-1}$ , and three characteristic absorption peaks which attributed to Chlorpyrifos located at the same position as in Figure 3 (a) in figure 3 (c). However, three characteristic absorption peaks of Abamectin at 1460.48  $\text{cm}^{-1}$ , 1112.64  $\text{cm}^{-1}$ , 982.49  $\text{cm}^{-1}$  and five characteristic

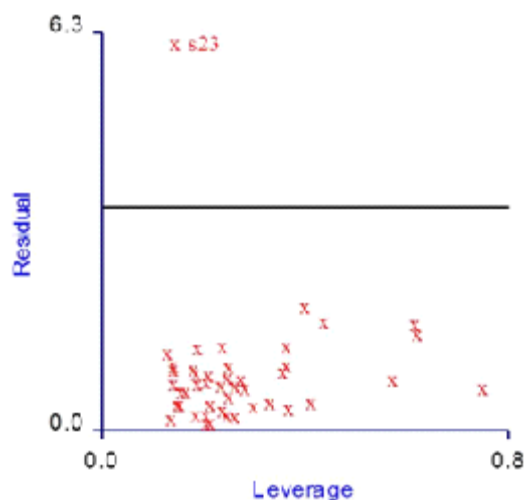


Fig. 7. Outliers test of MIR model

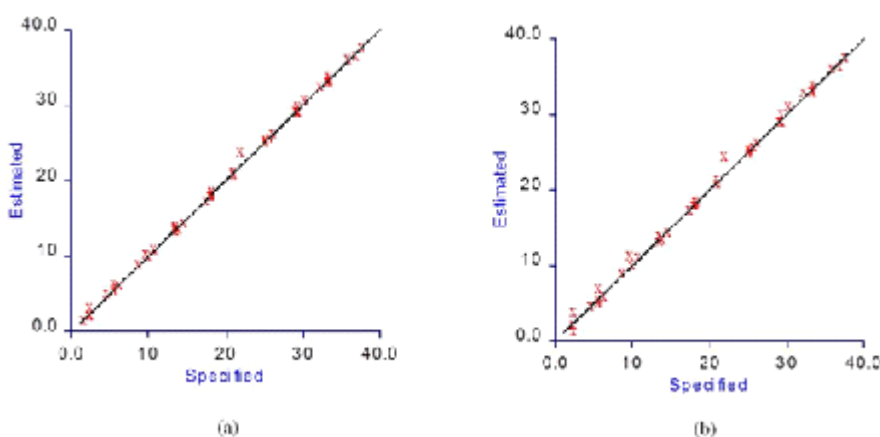


Fig. 8. The correlation of estimated and specified value of Chlorpyrifos (a), The related relationship figure of estimated value of validation set with the specified value of Chlorpyrifos (b)

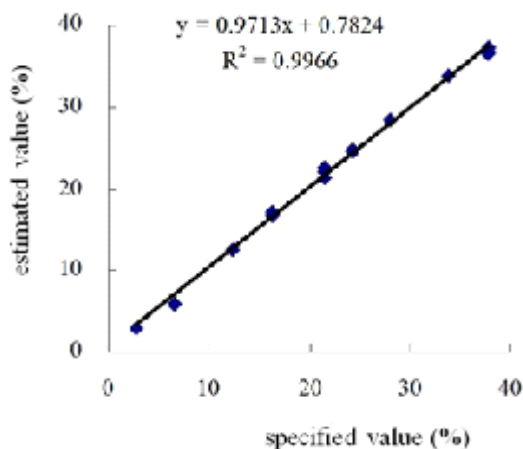


Fig. 9. The related relationship figure of the specified value with the estimated value for Chlorpyrifos content

absorption peaks of Chlorpyrifos at 1411.97  $\text{cm}^{-1}$ , 1273.55  $\text{cm}^{-1}$ , 1161.15  $\text{cm}^{-1}$ , 838.54  $\text{cm}^{-1}$ , 739.95  $\text{cm}^{-1}$  were located in figure 3 (d). In addition, it was observed only one characteristic absorption peak which belonged to Abamectin at 1460.48  $\text{cm}^{-1}$  and six characteristic absorption peaks of Chlorpyrifos located at 1409.61  $\text{cm}^{-1}$ , 1273.55  $\text{cm}^{-1}$ , 1161.15  $\text{cm}^{-1}$ , 973.03  $\text{cm}^{-1}$ , 838.54  $\text{cm}^{-1}$  and 739.95  $\text{cm}^{-1}$ .

Through the analysis of above five figures, both of the characteristic absorption peaks which belonged to Abamectin and Chlorpyrifos existed in five figures. The results showed that with the increase in the proportions of Chlorpyrifos solutions which was adulterated into Abamectin solutions, the number of characteristic absorption

peaks belonged to Abamectin constantly decreased. Conversely, the number of characteristic absorption peaks attributed to Chlorpyrifos gradually increased. However, one common characteristic absorption peaks of Abamectin at  $1460.48\text{ cm}^{-1}$ , three characteristic absorption peaks of Chlorpyrifos at  $1411.97\text{ cm}^{-1}$ ,  $1167.06\text{ cm}^{-1}$  and  $838.54\text{ cm}^{-1}$  were contained in five figures. The characteristic absorption peak which always existed can be identified as the existence of Abamectin and Chlorpyrifos. So it verified the feasibility of analyzing biological pesticides adulteration by using attenuated total reflection technique.

#### **The analysis of second derivative spectrum of Avermectin adulteration solution**

Second derivative spectrum was calculated to separate the overlapping peaks, reduce the peak superposition, improve the spectra resolution, enhance the information quality and highlight the spectra characteristics. And derivative spectrum can eliminate baseline drift or gentle background interference. Figure 4 (a), Figure 4 (b), Figure 4 (c), Figure 4 (d) and Figure 4 (e) were the second derivative spectra of 100 mg/L of Abamectin solutions adulterated with 10%, 20%, 30%, 40%, 50% 100 mg/L of Chlorpyrifos solutions. Comparing with Figure 3 (a), it added 2 characteristic absorption peaks in Figure 4 (a) which belonged to Abamectin at  $1708.94\text{ cm}^{-1}$  and  $868.91\text{ cm}^{-1}$ . Figure 4 (a) contained additionally three characteristic absorption peaks attributed to Chlorpyrifos at  $1413.16\text{ cm}^{-1}$ ,  $835.78\text{ cm}^{-1}$  and  $676.06\text{ cm}^{-1}$ . Comparing with Figure 3 (a), it added a characteristic absorption peak at  $676.06\text{ cm}^{-1}$  and reduced a characteristic absorption peak at  $1167.06\text{ cm}^{-1}$ . However, there were three characteristics absorption peaks in Figure 4 (b) which did not exist in Figure 3 (b). One characteristic absorption peak was reduced in which was in the presence of Figure 3 (b). At the same time, it increased five characteristic absorption peaks in Figure 4 (c) more than in Figure 3 (c). The two absorption peaks which belonged to Abamectin located at  $1708.94\text{ cm}^{-1}$  and  $868.91\text{ cm}^{-1}$ . The remaining three characteristic absorption peaks of Chlorpyrifos at  $916.24\text{ cm}^{-1}$ ,  $794.37\text{ cm}^{-1}$  and  $671.33\text{ cm}^{-1}$ . And one characteristic absorption peak of Chlorpyrifos was also reduced at  $1167.06\text{ cm}^{-1}$ . Contrasting Figure 3 (a) with Figure 4 (d), Figure 4 (d) was an increase of

two characteristic absorption peaks at  $1708.94\text{ cm}^{-1}$ ,  $1053.48\text{ cm}^{-1}$  and a decrease of one characteristic absorption peak at  $1460.48\text{ cm}^{-1}$  of Abamectin. It increased four characteristic absorption peaks at  $1332.70\text{ cm}^{-1}$ ,  $912.69\text{ cm}^{-1}$ ,  $794.37\text{ cm}^{-1}$ ,  $671.33\text{ cm}^{-1}$  and decreased one characteristic absorption peak at  $1273.55\text{ cm}^{-1}$  of Chlorpyrifos. Meanwhile, it increased eight characteristic absorption peaks in Figure 4 (e) more than in Figure 3 (e) and decreased two characteristic absorption peaks.

The derivative spectrum not only eliminated the interference of baseline drift or gentle, but also provided higher resolution capability more than original spectrum, sharper spectral profile and more abundant information. Some peaks were not significant in the original spectrum that could be clearly apparent in the second derivative spectrum. There were three characteristic absorption peaks belonged to Abamectin at  $1708.94\text{ cm}^{-1}$ ,  $1116.19\text{ cm}^{-1}$ ,  $1053.48\text{ cm}^{-1}$  and three characteristic absorption peaks attributed to Chlorpyrifos at  $1409.61\text{ cm}^{-1}$ ,  $835.78\text{ cm}^{-1}$ ,  $676.06\text{ cm}^{-1}$  in five figures, in common. For actual detection, as long as the several characteristic absorption peaks existed, it could serve as preliminary distinguish basis of Abamectin which adulterated Chlorpyrifos. It provided feasibility and validity of analyzing biological pesticides adulteration by ATR-FTIR technology for the further research.

#### **Comparison analysis of peak intensity of Avermectin adulteration solution**

Figure 5 (a), Figure 5 (b), Figure 5 (c), Figure 5 (d) and Figure 5 (e) were the IR spectra of 100 mg/L of Abamectin solutions adulterated with 10%, 20%, 30%, 40%, 50% 100 mg/L of Chlorpyrifos solutions in turn. According to above analysis of 2.1.1, it indicated that the characteristic absorption peaks attributed to Abamectin located at  $1460.48\text{ cm}^{-1}$ ,  $1112.64\text{ cm}^{-1}$ ,  $1051.12\text{ cm}^{-1}$  and  $990.46\text{ cm}^{-1}$ , but the characteristic absorption peaks attributed to Chlorpyrifos located at  $1411.97\text{ cm}^{-1}$ ,  $1273.55\text{ cm}^{-1}$ ,  $1161.15\text{ cm}^{-1}$ ,  $973.03\text{ cm}^{-1}$ ,  $838.72\text{ cm}^{-1}$  and  $739.95\text{ cm}^{-1}$  in Figure 5.

It obtained the following conclusions according to the changes of characteristic absorption peaks from analyzing Figure 5, the peak shape and peak intensity of characteristic absorption peak of Abamectin at  $1460.48\text{ cm}^{-1}$  gradually became gentle and weak with the

decrease in the content of Avermectin (such as shown by the arrow). On the contrary, the peak shape and peak intensity of the characteristic absorption peaks of Chlorpyrifos at  $1411.97\text{ cm}^{-1}$ ,  $1161.15\text{ cm}^{-1}$  and  $838.72\text{ cm}^{-1}$  became sharp and strong with the increase in the content of Chlorpyrifos (such as shown by the arrow). In addition, the peak intensity of the characteristic absorption peaks at  $1112.64\text{ cm}^{-1}$  and  $990.46\text{ cm}^{-1}$  weakened gradually. The above two characteristic absorption peaks disappeared when Abamectin solutions adulterated with 50% Chlorpyrifos solutions. When Abamectin solutions adulterated with 30%, 40% Chlorpyrifos solutions, the characteristic absorption peaks at  $1273.55\text{ cm}^{-1}$  and  $739.95\text{ cm}^{-1}$  appeared. And with the increase in the proportions of Chlorpyrifos which was adulterated into Abamectin, the peak intensity gradually strengthened. A characteristic absorption peak of Chlorpyrifos at  $973.03\text{ cm}^{-1}$  appeared when the proportion of Chlorpyrifos reached 50%.

These conclusions proved that with the increase in the proportions of Chlorpyrifos which was adulterated into Abamectin, the number of characteristic absorption peaks attributed to Abamectin dwindled. Instead, the amount of characteristic absorption peaks belonged to Chlorpyrifos increased. And it illustrated that with the increase in the proportions of Chlorpyrifos, its own peak intensity gradually strengthened, and the peak intensity of Avermectin gradually weakened.

#### **Similarity compare of Avermectin adulteration solution**

The similarity compare is a qualitative analysis method which is used to calculate the similarity degree between samples. Its principle is based on the mathematical correlation coefficient. The similarity degree is compared between two infrared spectra (or between a series of spectra and a spectral). In this study, the spectrum of 100 mg / L of Avermectin solutions was as standard. It examined the similarity between 100 mg / L of Avermectin solutions and 100 mg / L of Avermectin solutions adulterated with 10%, 20%, 30%, 40%, 50% 100 mg / L of Chlorpyrifos solutions. Similarity values were 0.8787, 0.6965, 0.4481, 0.2521, 0.1691 in order. The similarity values were descended in turn between 100 mg / L of Avermectin solutions and 100 mg / L of Avermectin solutions adulterated

with 10%, 20%, 30%, 40%, 50% 100 mg / L of Chlorpyrifos solutions. The similarity value was 0.8787 when 10% 100 mg / L Chlorpyrifos solutions were adulterated. It represented the main performance characteristics of Avermectin. The feature of Avermectin weakened and the feature of Chlorpyrifos enhanced gradually with the increase in the proportion of Chlorpyrifos solutions, which illustrated that it detected Chlorpyrifos more easily.

#### **Quantitative analysis of biological pesticide adulteration by ATR-FTIR technology**

##### **The reproducibility of ATR-FTIR technology**

It collected ten spectra of Chlorpyrifos EC C repetitively and continuously (Fig. 6). It could be seen from figure 6 that the peak position, the peak shape and the peak intensity of characteristic peaks of Chlorpyrifos overlapped substantially completely. And the minimum similarity value was 0.9996. It was well seen that the reproducibility of determination was very good by ATR-FTIR technology. So it could satisfy the requirements of quantitative analysis.

##### **The quantitative model of biological pesticide adulteration**

The IR spectra of 47 samples which were prepared in section 1.4.2 of the experimental methods were as calibration set. It established the quantitative model of Avermectin EC adulterated with Chlorpyrifos EC by PLS method. The model was validated by full cross-validation method. The results of test of model abnormal values were shown in Figure 7. The sample points which simultaneously satisfied greater than two times of average leverage value and three times of average residual value were regarded as abnormal samples. So it could be seen there were no abnormal samples to be removed from figure 7.

The spectral pretreatment methods of mean center, smoothing, standard normalized, baseline correction were used to optimize the model. The parameters of final optimal modeling method was centralized (mean, mean) and 9 point smoothing by calculating. The results of optimization of model were shown in table 1. The optimal factor numbers were 11 by cross-validation and F-test. And the final model parameters were that  $R^2$ , RMSEC and RMSECV were 99.88%, 0.44 and 0.79, respectively. Figure 8 (a) and Figure 8 (b) were the related relationship figures of the estimated value of calibration set with the specified

value of Chlorpyrifos and the estimated value of validation set with the specified value of Chlorpyrifos.

#### External validation of quantitative model of biological pesticide adulteration

Seventeen samples of experimental methods were selected as an external validation set according to the order of concentration gradient of configured samples and the mixed method of Avermectin EC and Chlorpyrifos EC. The optimal pretreatment method in section 2.2.2 was used to build the model. In addition, the predicted values and specified values were compared. Figure 9 was the related relationship figure of predicted value with specified value. And the final model parameters were that  $R^2$  (%) and the RMSEP of external validation set were 99.66 and 0.7. The relative prediction error of 17 samples in external validation set was in the range of -7.5%-5.5%. It illustrated that the quantitative model of ATR-FTIR technology had a good adaptability.

#### CONCLUSIONS

In this study, rapid qualitative and quantitative determination of biological pesticide (Avermectin) adulterated with highly toxic pesticide (Chlorpyrifos) were completed by ATR-FTIR technology. The IR absorbance spectra, the second derivative spectra, the comparative analysis of peak intensity and similarity comparison were used for qualitative analysis. The results showed that with the increase in the proportions of Chlorpyrifos which was adulterated into Abamectin, the number of characteristic absorption peaks belonged to Abamectin decreased. And the peak intensity gradually weakened. Conversely, the number of characteristic absorption peaks attributed to Chlorpyrifos increased gradually. The peak intensity gradually strengthened. It represented the main performance characteristics of Avermectin when 10% Chlorpyrifos solutions were adulterated. The feature of Avermectin weakened and the feature of Chlorpyrifos enhanced gradually with the increase in the proportion of Chlorpyrifos solutions. In addition, the stability of the samples became worse gradually. The results of quantitative research showed that ATR-FTIR technology can accurately determine the content of Abamectin EC adulterated with Chlorpyrifos. And the specified values and the

estimated values were no significant differences.  $R^2$  (%), RMSEC, RMSECV and RMSEP were 99.88, 0.44, 0.79 and 0.70, respectively. It illustrated that the quantitative model of ATR-FTIR technology had a good adaptability. The method established by ATR-FTIR technology was feasible to qualitatively and quantitatively detect the biological pesticide of Abamectin adulterated with high toxic chemical pesticides of Chlorpyrifos. And the method had high precision. The detection methods of biological pesticides adulteration will be more perfect when this technology is combined with traditional detection methods (gas chromatography). It will make the detection methods of biological pesticides adulteration more perfect and reasonable. It has a great significance for quality control of pesticides and safety monitoring of agricultural product of supervision departments.

#### ACKNOWLEDGMENTS

This research was financially supported by Special Fund for Agro-scientific Research in the Public Interest, the Ministry of Agriculture of the People's Republic of China (201003008, 201203046) and Natural Science Foundation of China (31201125).

#### REFERENCES

1. Jorgensen S. E.. Applications in Ecological Engineering. In: *Conservation Biological Control and Biopesticides in Agricultural* (Wratten SD, ed). Amsterdam: Elsevier Press, 2008; pp 744-7.
2. Samuel Gan-Mor, Graham A. M. Recent Developments in Sprayers for Application of Biopesticides—an Overview. *Biosystems Engineering*, 2003; **84**(2): 119-25.
3. Albero B., Sánchez-Brunete C., Tadeo J. L. Determination of endosulfan isomers and endosulfan sulfate in tomato juice by matrix solid-phase dispersion and gas chromatography. *Journal of Chromatography A*, 2003; **1007**(1-2): 137-43.
4. Ionara R. P., René J. J. V., André de K., Rafael R., Samile M., Caroline A., Renato Z. Design of a compressed air modulator to be used in comprehensive multidimensional gas chromatography and its application in the determination of pesticide residues in grapes. *Journal of Chromatography A*, 2009; **1216**(15):

- 3305-11.
5. French A.G., Vidal J. L. M., López T. L., Aguado S. C., Salvador I. M. Monitoring multi-class pesticide residues in fresh fruits and vegetables by liquid chromatography with tandem mass spectrometry. *Journal of Chromatography A*, 2004; **1048**(2): 199-206.
  6. Cunha S. C., Fernandes J. O., Alves A., Oliveira M.B.P.P. Fast low-pressure gas chromatography-mass spectrometry method for the determination of multiple pesticides in grapes, musts and wines. *Journal of Chromatography A*, 2009; **1216**(1-2): 119-26.
  7. Qian G. L., Wang L. M., Wu Y. R., Zhang Q., Sun Q., Liu Y., Liu F. Q. A monoclonal antibody-based sensitive enzyme-linked immunosorbent assay (ELISA) for the analysis of the organophosphorous pesticides chlorpyrifos-methyl in real samples. *Food Chemistry*, 2009; **117**(2): 364-70.
  8. Campanella L., Bonanni A., Martini E., Todini N., Tomassetti M. Determination of triazine pesticides using a new enzyme inhibition tyrosinase OPEE operating in chloroform. *Sensors and Actuators B: Chemical*, 2005; 111-112: 505-14.
  9. Khanmohammadi M., Armenta S., Garrigues S., Guardia M. de la. Mid-and near-infrared determination of metribuzin in agrochemicals. *Vibrational Spectroscopy*, 2008; **46**(2): 82-8.
  10. Annette N., Gregor H., Rolf R. Efficient discrimination of oat and pea roots by cluster analysis of Fourier transform infrared (FTIR) spectra. *Field Crops Research*, 2010; **119**(1): 78-84.
  11. Xiao Y. L., Zhang P. X., Qian X. F. Micro-Raman and Fluorescence Spectra of Several Agrochemicals. *Spectroscopy and Spectral Analysis*, 2004; **24**(5): 579-81. (in Chinese)
  12. Armenta S., Quintás G., Garrigues S., Guardia M. de la. A validated and fast procedure for FTIR determination of Cypermethrin and Chlorpyrifos. *Talanta*, 2005; **67**(3): 634-9.
  13. Kang N., Kasemsumran S., Woo Y. A. Optimization of Informative Spectral Regions for the Quantification of Cholesterol, Glucose and Urea in Control Serum Solutions Using Searching Combination Moving Window Partial Least Squares Regression Method with Near Infrared Spectroscopy. *Chemometrics and Intelligent Laboratory Systems*, 2006; **82**(1-2): 90-6.
  14. Bastien P., Vinzi V. E., Tenenhaus M. PLS generalized linear regression. *Computational Statistics & Data Analysis*, 2005; **48**(1): 17-46.
  15. Xu L., Wang N. Y., Ba S. H., Wang Y. L. Application and Progress of Fourier Transform Attenuated Total Reflection Infrared Spectroscopy. *Spectroscopy and Spectral Analysis*, 2004; **24**(3): 317-9. (in Chinese)
  16. Gao X., Wang X. Y., Wang D., Hao X. H., Min S. G. Rapid Detection of Dichlorvos in Chlorpyrifos by Mid-Infrared and Near-Infrared Spectroscopy. *Spectroscopy and Spectral Analysis*, 2010; **30**(11): 2962-6. (in Chinese)
  17. Doran E. M., Yost M. G., Fenske R. A. Measuring Dermal Exposure to Pesticide Residues with Attenuated Total Reflectance Fourier Transform Infrared (ATR-FTIR) Spectroscopy. *Bulletin of Environmental Contamination and Toxicology*, 2000; **64**(5): 666-72.
  18. Suo J. X., Sun S. Q., Wang W. Q. Application of FTIR Spectroscopy to the Identification of Glycyrrhiza Uralensis Fisch. *Spectroscopy and Spectral Analysis*, 2010; **30**(5): 1218-23. (in Chinese)
  19. Roza-Delgado B., de la, Soldado A., Martí'nez-Fernández A., Vicente F., Garrido-Varo A., Pe' rez-Marl' n D., Haba M. J. de la, Guerrero-Ginel J. E. Application of near-infrared microscopy (NIRM) for the detection of meat and bone meals in animal feeds: A tool for food and feed safety. *Food Chemistry*, 2007; **105**: 1164-70.
  20. Wu X. H., Chen D. Z. Recent Development of Non-linear Partial Least Squares in Chemometrics. *Chinese Journal of Analytical Chemistry*, 2004; **32**(4): 534-40. (in Chinese)
  21. Lu W. Z., Yuan H. F., Xu G. D. (ed): Modern Near Infrared Spectroscopy Analytical Technology. Beijing, China Petrochemical Press, 2000; pp 141-150. (in Chinese)
  22. Liang Y. Z., Jiang J. H. Spectral Regions Selection to Improve Prediction Ability of PLS Models by Changeable Size Moving Window Partial Least Squares and Searching Combination Moving Window Partial Least Squares. *Anal. Chem.*, 2004; **501**(2): 183-91.
  23. Xu R., Sun S. Q., Liu Y. G., Chen J., Liu T. N., Chen S. L. FTIR and 2D-IR Spectroscopic Studies on Different Sources of Herba Cistanche. *Spectroscopy and Spectral Analysis*, 2010; **30**(12): 897-900. (in Chinese)
  24. Xu L., Wang N. Y. Comparative Study on ATR/FTIR Technology and Infrared Transmission Method for the Determination of Pesticides in Vegetables. *Infrared Technology*, 2008; **30**(12): 702-5. (in Chinese)
  25. Syetov Y., Vdovin A. Infrared spectra of benzoxazoles exhibiting excited state proton transfer. *Vibrational Spectroscopy*, 2010; **53**(1): 146-50.